Brief Communications

ATP Hydrolysis Is Critically Required for Function of $Ca_V1.3$ Channels in Cochlear Inner Hair Cells via Fueling Ca^{2+} Clearance

Simon Weiler,[1,2] Stefanie Krinner,[1,3] Aaron B. Wong,[1,4] Tobias Moser,[1,2,3,4] and Tina Pangršič[1,4]

[1]InnerEarLab, Department of Otolaryngology, University Medical Center Göttingen, 37099 Göttingen, Germany, [2]International Max-Planck Research School Neuroscience, Göttingen Graduate School for Neuroscience and Molecular Biosciences, and [3]International Max-Planck Research School Molecular Biology, Göttingen Graduate School for Neuroscience and Molecular Biosciences, University of Göttingen, 37077 Göttingen, Germany, and [4]Collaborative Research Center 889, University of Göttingen, 37099 Göttingen, Germany

Sound encoding is mediated by Ca^{2+} influx-evoked release of glutamate at the ribbon synapse of inner hair cells. Here we studied the role of ATP in this process focusing on Ca^{2+} current through $Ca_V1.3$ channels and Ca^{2+} homeostasis in mouse inner hair cells. Patch-clamp recordings and Ca^{2+} imaging demonstrate that hydrolyzable ATP is essential to maintain synaptic Ca^{2+} influx in inner hair cells via fueling Ca^{2+}-ATPases to avoid an increase in cytosolic $[Ca^{2+}]$ and subsequent Ca^{2+}/calmodulin-dependent inactivation of $Ca_V1.3$ channels.

Key words: **calcium; calmodulin; channel; hair cell; inactivation; ribbon synapse**

Introduction

Neurotransmission at the inner hair cell (IHC) synapse is driven by Ca^{2+} influx (I_{Ca}) through $Ca_V1.3$ channels (Platzer et al., 2000; Brandt et al., 2003; Dou et al., 2004) that cluster at the active zones (AZs) (Brandt et al., 2005). Within IHCs, this L-type channel activates at low voltage and displays only weak Ca^{2+} dependent inactivation (CDI) (Yang et al., 2006; Cui et al., 2007). At least two mechanisms of inhibiting CDI (Lee et al., 1999; Peterson et al., 1999) of $Ca_V1.3$ in IHCs are currently considered: (1) autoregulation involving the distal and proximal C-terminal domains (Singh et al., 2008) and (2) competition of Ca^{2+} binding proteins (CaBPs) with calmodulin (Yang et al., 2006; Cui et al., 2007; Schrauwen et al., 2012). However, a unifying picture of CDI regulation during physiological signaling in IHCs has yet to be established.

Here we studied the role of ATP in Ca^{2+} signaling and $Ca_V1.3$ channel regulation in IHCs. Decay ("rundown") of I_{Ca} is commonly observed in whole-cell patch-clamp recordings, suggesting a failure of the channel regulation and/or function upon washout of cell constituents. Adding ATP to the pipette can partially prevent I_{Ca} rundown (Chad and Eckert, 1986; Armstrong and Eckert, 1987). Besides being used by kinases and phosphatases, ATP supports the function of ATP-driven pumps and is therefore required for cellular Ca^{2+} homeostasis and low basal $[Ca^{2+}]_i$ (for review, see Mammano et al., 2007). Elevations in basal $[Ca^{2+}]_i$ could affect the Ca^{2+} channel behavior (e.g., via CDI). The regulation of $[Ca^{2+}]$ at ribbon synapses involves Ca^{2+} buffering and diffusion (Roberts, 1993; Tucker and Fettiplace, 1995; Issa and Hudspeth, 1996; Frank et al., 2009) as well as Ca^{2+} clearance via Ca^{2+} ATPase (PMCA) and Na^+/Ca^{2+} exchange (Zenisek and Matthews, 2000; Kennedy, 2002).

Here, we combined patch-clamp recordings and Ca^{2+} imaging of IHCs during dialysis with different [ATP] or the poorly hydrolyzable analog ATP-γ-S to probe the requirement of ATP hydrolysis for Ca^{2+} homeostasis and $Ca_V1.3$ channel regulation. We demonstrate that interference with ATP hydrolysis dramatically increases $[Ca^{2+}]_i$ because of failure of PMCA-mediated Ca^{2+} clearance and consequently decreases the presynaptic I_{Ca} via Ca^{2+}/calmodulin-mediated CDI.

Materials and Methods

Electrophysiology. IHCs from the apical coil of organs of Corti from C57 Bl/6 mice of either sex (postnatal day 14 [P14] to P16) were patch-clamped (at 20°C–25°C) as described previously (Moser and Beutner, 2000). The pipette solution contained the following (in mM): 134–140 Cs-gluconate, 10 tetraethylammonium-Cl (TEA-Cl), 10 4-AP, 10 CsOH-HEPES, 1 $MgCl_2$, 0.3 NaGTP, 0.5 or 10 EGTA or 10 BAPTA and 0–4 MgATP or 2 Li_4-ATP-γ-S, pH 7.2, osmolarity: 295 mOsm/L. CaMKII 290–309, H-89 (both Merck), carboxyeosin, trifluorocarbonylcyanide phenylhydrazone (FCCP) (both Sigma-Aldrich), and fura-2 and Fluo-4FF (both Invitrogen) were dissolved in H_2O. KN-93, CaMKII inhibitor

Received Nov. 27, 2013; revised March 14, 2014; accepted April 6, 2014.

Author contributions: S.W., T.M., and T.P. designed research; S.W. and S.K. performed research; S.W., S.K., and A.B.W. analyzed data; S.W., T.P., and T.M. wrote the paper.

This work was supported by the German Research Foundation through the priority program 1608 to T.M. and the collaborative research center 889 project A2 to T.M. We thank S. Gerke and C. Senger-Freitag for expert technical assistance and Lars Maier for providing CBD and KN-93.

The authors declare no competing financial interests.

Correspondence should be addressed to either of the following: Dr. Tina Pangršič, Synaptic Physiology of Mammalian Vestibular Hair Cells Junior Research Group, InnerEarLab, Department of Otolaryngology, University Medical Center Göttingen, 37099 Göttingen, Germany, E-mail: tpangrs@gwdg.de; or Dr. Tobias Moser, InnerEarLab, Department of Otolaryngology and Collaborative Research Center 889, University Medical Center Göttingen, 37099 Göttingen, Germany, E-mail: tmoser@gwdg.de.

S. Weiler's present address: Max Planck Institute of Neurobiology, Am Klopferspitz 18, D-82152 Martinsried, Germany.

T. Pangršič's present address: Synaptic Physiology of Mammalian Vestibular Hair Cells Junior Research Group, InnerEarLab, Dept. of Otolaryngology, University Medical Center Göttingen, 37099 Göttingen, Germany.

DOI:10.1523/JNEUROSCI.4990-13.2014

 0270-6474/14/346843-06$15.00/0

XII, KT5720 (all Merck), CGS-9343B (Sigma-Aldrich), and berbamine E_6 (Santa Cruz Biotechnology) were dissolved in DMSO. The extracellular solution contained the following (in mM): 110 NaCl, 35 TEA-Cl, 10 HEPES, 1 CsCl, 1 $MgCl_2$, 2 $CaCl_2$, 11.1 glucose, pH 7.2, osmolarity: 300 mOsm/L. BayK 8644 (Biotrend) was added to the extracellular solution. The liquid junction potential was numerically estimated as 14 mV and subtracted. Leak currents were subtracted using the P/10 protocol. The series resistance was typically <15 MΩ.

Camera-based Ca^{2+} imaging. IHCs were loaded with 100 μM fura-2 and imaged alternately at 340 and 380 nm using a polychrome IV light source and an Imago VGA CCD operated by Tillvision software (all, Tillphotonics-FEI). Fura-2 measurements were calibrated *in vivo* and *in vitro* (Neher, 2013), and $[Ca^{2+}]$ was calculated according to the following equation (Grynkiewicz et al., 1985):

$$[Ca^{2+}]_i = K_{eff}(R - R_{min})/(R_{max} - R).$$

In our experiments, calibration coefficients determined *in vivo* were $R_{min} = 0.24$, $R_{max} = 5.15$, and $R_{med} = 1$ (yielding K_{eff} of 2457 nM). The K_D for fura-2 was found to be 243.5 nM.

Confocal Ca^{2+} imaging. Confocal Ca^{2+} imaging was performed using an Olympus FV300 confocal microscope essentially as described previously (Frank et al., 2009) using 400 μM Fluo-4FF in the pipette solution described above. In brief, carboxytetramethyl-rhodamine-conjugated RIBEYE-binding dimer peptide (10 μM) (Francis et al., 2011) was used to identify synaptic ribbons, and changes in Fluo-4FF (400 μM) fluorescence were repeatedly observed with line scans through the center of the same ribbon during (20 ms) depolarizations to −7 mV.

Data analysis and statistics. Data analysis and statistics were done in IgorPro and MATLAB. Wilcoxon rank test was used to compare data (with non-normal distribution and/or unequal variances). Correlation was tested using Pearson's correlation. Regression lines were compared among each other by one-way analysis of covariance (ANCOVA) test. Data are presented as mean ± SEM.

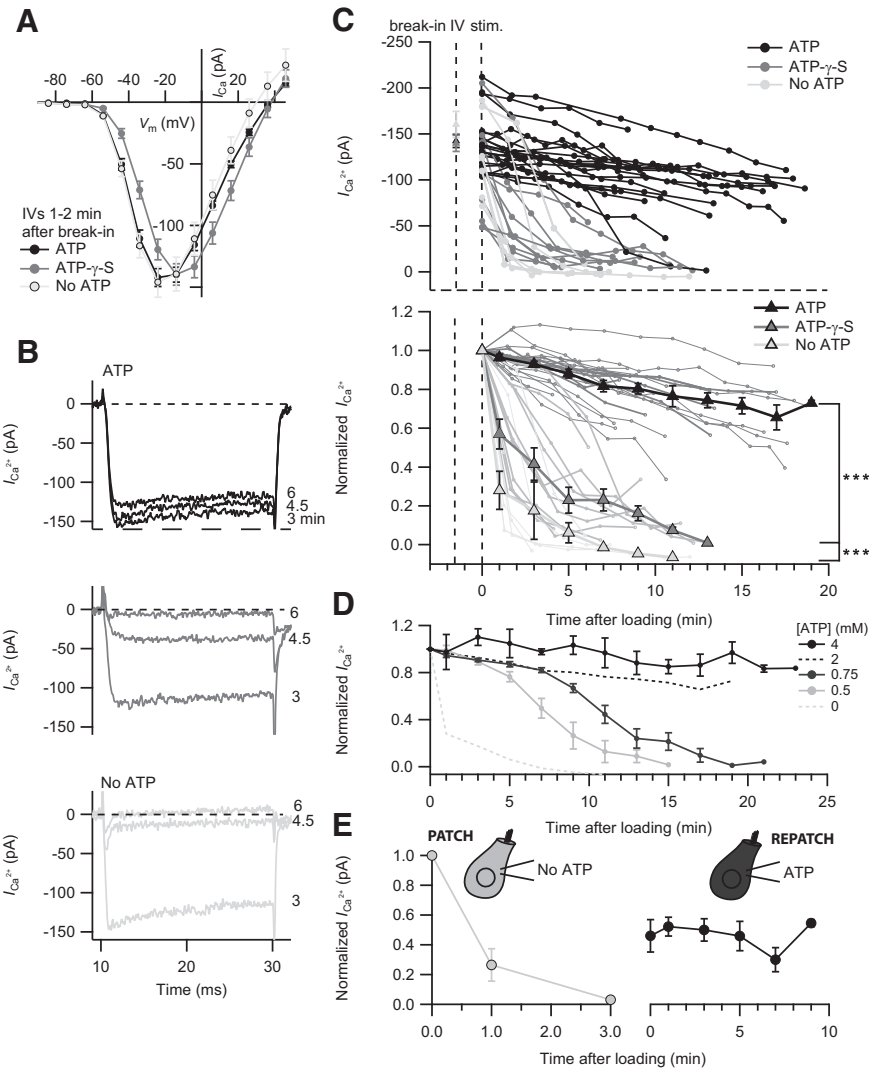

Figure 1. ATP hydrolysis is required for maintaining IHC I_{Ca}. ***A***, Unaltered amplitude of I_{Ca} revealed by the current–voltage relationship (IV) of IHCs dialyzed with 2 mM ATP ($n = 26$), 2 mM ATP-γ-S ($n = 15$), or without exogenous ATP ($n = 8$) at 1–2 min after break-in. ***B***, Representative I_{Ca} in response to 20 ms depolarization to peak I_{Ca} potential after 3, 4.5, and 6 min dialysis with ATP, ATP-γ-S, or without ATP. ***C***, Time course of the I_{Ca} reduction upon ATP manipulation. Top, The I_{Ca} of individual IHCs dialyzed with ATP ($n = 21$), ATP-γ-S ($n = 13$), or without ATP ($n = 8$). Bottom, I_{Ca} normalized to the first 20 ms depolarization of each cell. Mean normalized values with SEM displayed as overlay that were binned by time, with a bin size of 120 s. Statistical comparison was performed between 1 min and 11 min after loading. ***D***, The concentration-dependent effect of ATP on Ca^{2+} channels. Normalized I_{Ca} values of IHCs dialyzed with 0.5 ($n = 4$), 0.75 ($n = 5$), or 4 mM ATP ($n = 5$) over time. For comparison, the mean normalized I_{Ca} values of IHCs dialyzed with 2 mM (black dashed line) and without ATP (gray dashed line) are displayed. ***E***, The I_{Ca} rundown is partially reversible. IHCs initially infused without ATP ($n = 3$) were repatched with a solution containing 2 mM ATP after 8–13 min. ***$p < 0.001$.

Results

IHC $Ca_V1.3$ channels require hydrolyzable ATP for proper function

To determine the requirement of ATP for Ca^{2+} influx, IHCs were dialyzed with 2 mM ATP, ATP-γ-S, or pipette solution lacking ATP. We first assessed the I_{Ca} properties (current–voltage relationship, IV) 1–2 min after break-in (Fig. 1*A*) and thereafter ran a series of depolarization pulses (P1–P3, 20 ms; P4, 100 ms) to the peak I_{Ca} potential. Taking into account the molecular weight (MW), series resistance R_S, and the estimated cell volume of 2.2 pl, the diffusion time constant for ATP (MW = 507.18 g/mol, $R_S = 12$ MΩ) and ATP-γ-S (MW = 546.98 g/mol, $R_S = 10$ MΩ) was calculated as 67 and 57 s, respectively (Pusch and Neher, 1988). Based on these calculations, the diffusional exchange should have been complete after 3–4 min, when P1 was applied. The cells infused with ATP-γ-S or 0 ATP may not have been completely devoid of ATP because of further ATP supply by oxidative metabolism, glycolysis, or phosphocreatine.

The initial IVs revealed comparable I_{Ca} amplitudes, reflecting the largely unaltered physiological state of the IHCs briefly after break-in. IHCs dialyzed with ATP-γ-S displayed a significantly faster rundown of I_{Ca} compared with controls with 2 mM ATP in the pipette ($p < 0.001$; Fig. 1*B*,*C*). For better comparison, I_{Ca} values were normalized to the response upon P1 (Fig. 1*C*). Without exogenous ATP or ATP-γ-S, the I_{Ca} rundown was even more pronounced ($p < 0.001$ for comparison to ATP-γ-S; Fig. 1*B*,*C*). Interestingly, 4 mM ATP in the pipette prevented the mild rundown observed with 2 mM ATP (Fig. 1*D*). On the contrary, lowering [ATP] below 2 mM caused the onset of a fast rundown after a few minutes (Fig. 1*D*).

We then tested whether the effects of the lack of hydrolyzable ATP on Ca^{2+} channels is reversible. IHCs were initially dialyzed

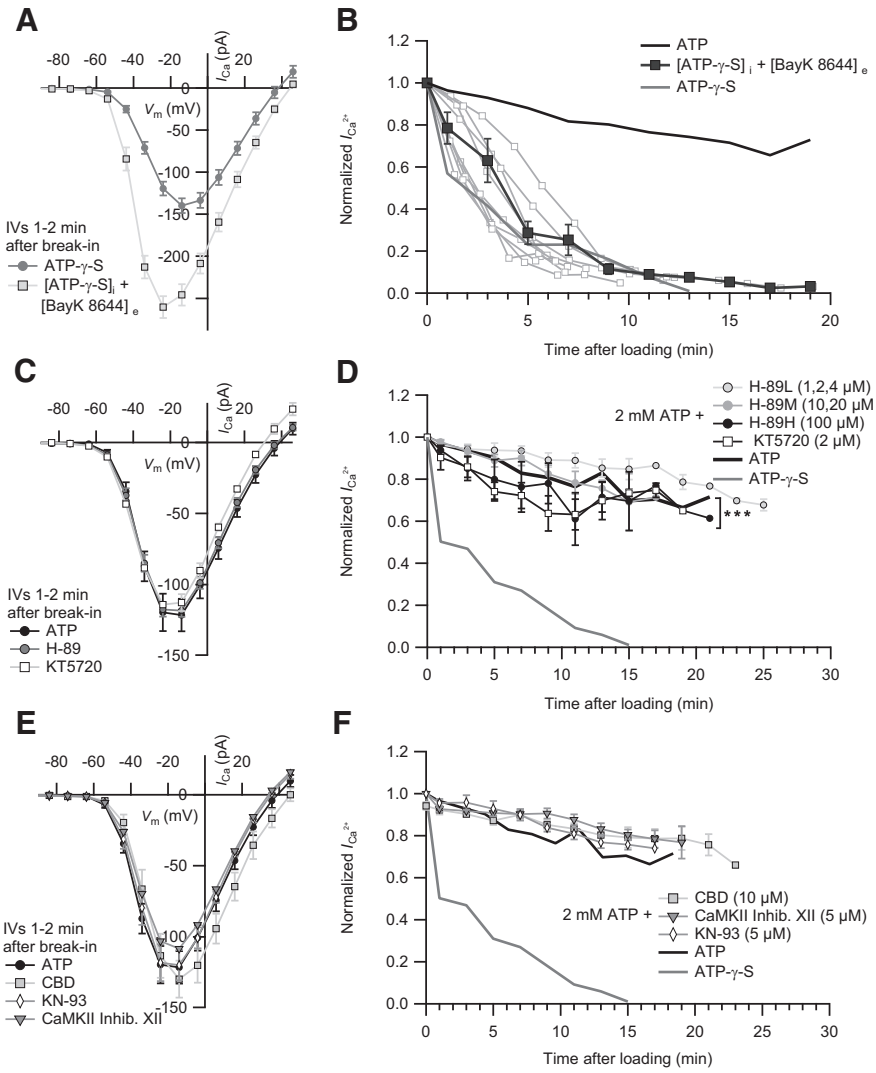

Figure 2. Probing the requirement of IHC I_{Ca} for phosphorylation by PKA and CaMKII. ***A***, The IV of IHCs dialyzed with ATP-γ-S in the absence ($n = 15$) and presence of 5 μM extracellular BayK 8644 ($n = 15$). ***B***, BayK 8644 did not significantly prevent the I_{Ca} rundown ($p = 0.43$, statistical comparison was performed between 1 min and 13 min after loading). Mean normalized I_{Ca} values of IHCs dialyzed with ATP-γ-S ($n = 13$) in the presence of BayK 8644 ($n = 9$). For comparison, we display the mean normalized I_{Ca} of IHCs dialyzed with ATP. ***C***, The effect of PKA inhibition on IHC I_{Ca}. The IVs of IHCs dialyzed with ATP in the absence ($n = 5$) or presence of intracellular H-89 ($n = 14$) or KT5720 ($n = 5$) are comparable. ***D***, The normalized mean I_{Ca} values of IHCs dialyzed with low (1, 2, and 4 μM, $n = 6$), middle (10 and 20 μM, $n = 5$), or high (100 μM, $n = 3$) concentration of H-89 or KT5720 (2 μM, $n = 6$) over time. Statistical comparison was performed between 3 min and 19 min after loading. ***E***, CaMKII inhibition shows no effect on IHC I_{Ca}. The IVs of IHCs dialyzed with ATP in the absence ($n = 5$) or presence of intracellular CBD ($n = 4$), CaMKII Inhibitor XII ($n = 3$), or KN-93 ($n = 4$). ***F***, The rundown of the mean normalized I_{Ca} in IHCs dialyzed with CBD ($n = 4$), inhibitor XII ($n = 4$), and KN-93 ($n = 3$) is similar to controls. In comparison, the mean normalized I_{Ca} of IHCs dialyzed with ATP or ATP-γ-S is displayed. ***$p < 0.001$.

with a solution lacking ATP, the pipette was gently pulled off enabling resealing of the IHC membrane, and the cell was then repatched with an internal solution containing 2 mM ATP after 8–13 min (Fig. 1*E*). As observed, I_{Ca} could partially be restored and remained stable over another 10 min. Similar results were obtained in IHCs initially dialyzed with ATP-γ-S (data not shown).

Finally, we examined the effects of DHP agonist BayK 8644 on the I_{Ca} of ATP-γ-S-treated IHCs because BayK 8644 has been shown to partially overcome inhibition of I_{Ca} by lack of hydrolyzable ATP in pituitary GH_3 and smooth muscle cells (Armstrong and Eckert, 1987; Ohya and Sperelakis, 1989). We observed a twofold increase in the maximum steady-state I_{Ca} amplitude of the initial IV (Fig. 2*A*) consistent with the augmenting effects of BayK 8644 on IHC $Ca_V1.3$ channels (Brandt et al., 2005). However, regardless of BayK 8644, ATP-γ-S still caused a significant rundown of I_{Ca} ($p = 0.43$, compared with 2 mM ATP-γ-S without BayK 8644; Fig. 2*B*).

Probing for a role of phosphorylation in the regulation of IHC $Ca_V1.3$ channels

Because ATP requirement may reflect phosphorylation events relevant to Ca^{2+} channel function, we tested for effects of the protein kinase A (PKA) inhibitors H-89 (Chijiwa et al., 1990) and KT5720 (Okada et al., 1995), and the calmodulin-dependent kinase II inhibitors CamKII 290–309 (calmodulin binding domain [CBD]) (Basavappa et al., 1999), CaMKII Inhibitor XII (Asano et al., 2010), and KN-93 (Sumi et al., 1991) applied via the pipette that also contained 2 mM ATP. Micromolar concentrations of drugs (see figure legends; K_i or IC_{50} values in nM range) were chosen after observing no effects at submicromolar levels. None of the tested PKA or CaMKII inhibitors had an effect on the IV (Fig. 2*C*,*E*). Of all the kinase inhibitors (Fig. 2*D*,*F*), only KT5720 had an effect on the I_{Ca} measurements compared with control ($p < 0.001$).

Correlation between the rise of basal $[Ca^{2+}]_i$ and Ca^{2+} current rundown

Next, we considered the possibility that the lack of hydrolyzable ATP disables Ca^{2+} pumping and thereby Ca^{2+} clearance. Using simultaneous fura-2 imaging of $[Ca^{2+}]_i$ and whole-cell I_{Ca} recordings in IHCs dialyzed with ATP-γ-S (and 0.5 mM EGTA), we found that the I_{Ca} reduction coincided with a rise of basal $[Ca^{2+}]_i$ (Fig. 3*A*,*B*). Furthermore, IHCs that displayed a fast and pronounced elevation of basal $[Ca^{2+}]_i$ also displayed the most severe I_{Ca} rundown (Fig. 3*B*, dashed lines), also reflecting in the observed negative correlation between the rise of basal $[Ca^{2+}]_i$ and the I_{Ca} (Fig. 3*D*).

We then tested whether the PMCAs are the main mechanism of ATP-dependent Ca^{2+} clearance and required for maintaining Ca^{2+} influx in IHCs. Application of the PMCA inhibitor carboxyeosin (CE) caused a rise of the basal $[Ca^{2+}]_i$ and a parallel decrease of I_{Ca} (Fig. 3*A*,*C*,*D*). Once again, the IHCs with the fastest and largest elevation of basal $[Ca^{2+}]_i$ displayed the most severe I_{Ca} rundown. We conclude that failure of PMCA-mediated Ca^{2+} clearance explains most of the I_{Ca} reduction observed in the presence of ATP-γ-S. The slope of the regression line of cells dialyzed without ATP was steeper than of the cells containing ATP-γ-S ($p = 0.0012$), suggesting the contribution of an addi-

tional ATP-dependent mechanism to maintenance of I_{Ca} that can use ATP-γ-S.

To test for a direct role of mitochondria in Ca^{2+} homeostasis and regulation of Ca^{2+} influx, the uncoupling agent FCCP was used. The combined application of FCCP and CE resulted in an elevation of $[Ca^{2+}]$ and corresponding Ca^{2+} current rundown similar to the one observed with CE alone. However, the slope of the regression line of I_{Ca} and basal $[Ca^{2+}]_i$ was significantly steeper in the IHCs treated with CE and FCCP compared with either CE or ATP-γ-S ($p = 0.0007$ for ATP-γ-S, $p = 0.002$ for CE vs ATP + CE + FCCP, ANCOVA), suggesting that application of FCCP enhances Ca^{2+} channel inactivation potentially via disruption of mitochondrial ATP generation and/or Ca^{2+} uptake affecting the clearance of synaptic Ca^{2+}.

Ca^{2+}/calmodulin-mediated CDI of Ca^{2+} channels underlies the I_{Ca} rundown in the absence of hydrolyzable ATP

The most parsimonious interpretation of the I_{Ca} reduction caused by ATP-γ-S or CE is an increased CDI of Ca^{2+} channels resulting from the elevated resting $[Ca^{2+}]_i$. To test this hypothesis, we studied the effect of adding a high concentration (10 mM) of the Ca^{2+} chelators EGTA or BAPTA to the ATP-γ-S-containing pipette solution. In both cases, the pronounced global rise in $[Ca^{2+}]_i$ as well as the I_{Ca} reduction were prevented (Fig. 4*A*,*C*).

We further tested the hypothesis of an increased Ca^{2+}/calmodulin-mediated CDI by applying the calmodulin inhibitors E_6 berbamine (Grant and Fuchs, 2008) and CGS-9343B (Norman et al., 1987). They significantly slowed down I_{Ca} rundown despite a comparable increase of the resting $[Ca^{2+}]$ (Fig. 4*B*,*C*), further supporting our notion that the lack of hydrolyzable ATP reduces the IHC I_{Ca} via a rise in resting $[Ca^{2+}]$ and consecutive CDI of the Ca^{2+} channels.

Finally, to test how the lack of ATP affects synaptic Ca^{2+} signals, we combined patch-clamp and confocal Ca^{2+} imaging that allows spatiotemporal characterization of submicrometer-sized Ca^{2+} domains at the fluorescently tagged ribbon-type AZs (Frank et al., 2009). We observed that the synaptic Ca^{2+} domains rapidly disappeared in the absence of ATP from the pipette solution, correlating in time with the rundown of whole-cell I_{Ca} (Fig. 4*D*,*E*).

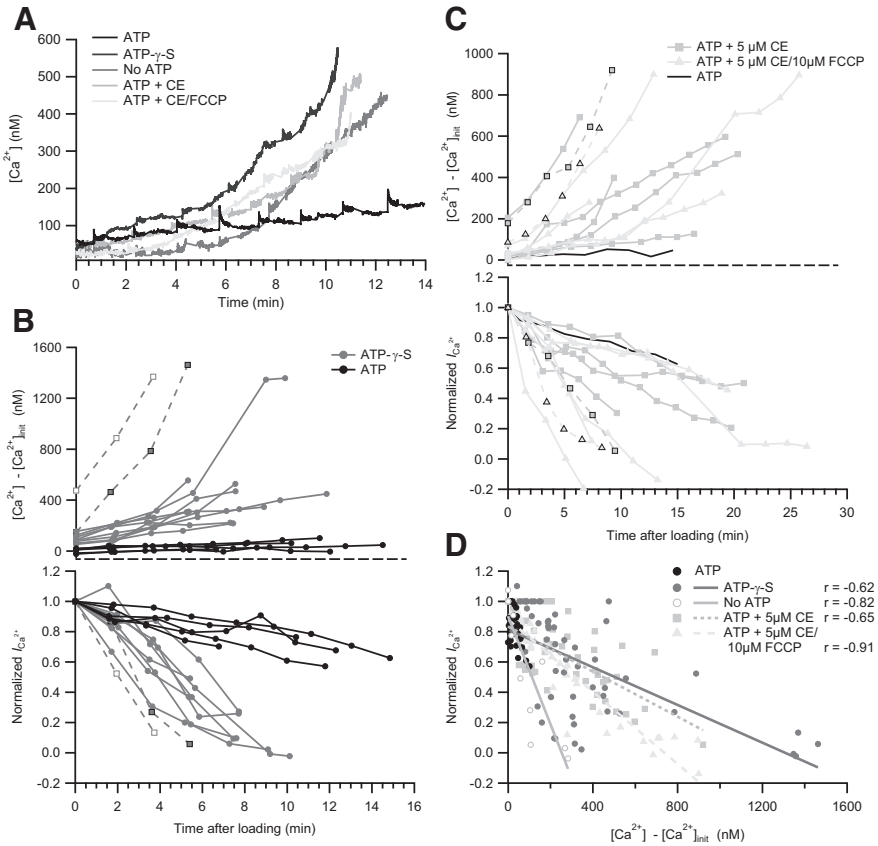

Figure 3. IHC I_{Ca} requires intact Ca^{2+} homeostasis. ***A***, Representative examples of IHC bulk $[Ca^{2+}]_i$ obtained by fura-2 imaging under different conditions: with 2 mM ATP, 2 mM ATP-γ-S, no ATP, 2 mM ATP + 10 µM CE, or 2 mM ATP + 5 µM CE + 10 µM FCCP. In each case, the pipette contained 0.5 mM EGTA. ***B***, Simultaneous measurements of $[Ca^{2+}]$ and the normalized I_{Ca} of single IHCs dialyzed with 2 mM ATP ($n = 5$) or 2 mM ATP-γ-S ($n = 11$). The initial $[Ca^{2+}]$ ($[Ca^{2+}]_{init}$) measured after sufficient loading of fura-2 was subtracted from subsequent $[Ca^{2+}]$ measurements. Dotted lines indicate two ATP-γ-S-cells with corresponding $[Ca^{2+}]_i$ values and I_{Ca}. ***C***, Simultaneous measurements of $[Ca^{2+}]$ and the normalized I_{Ca} of single IHCs dialyzed with 2 mM ATP + 5 µM CE ($n = 6$) or with 2 mM ATP + 5 µM CE + 10 µM FCCP ($n = 6$). For comparison, the mean $[Ca^{2+}]_i$ of control IHCs (no drug) is shown ($n = 5$). ***D***, $[Ca^{2+}]_i$ and I_{Ca} rundown are correlated for IHCs dialyzed with ATP-γ-S, no ATP ($n = 3$), ATP + CE, or ATP + CE + FCCP. Pearson correlation coefficient (r) and regression lines are displayed. There are different slopes for no ATP and ATP-γ-S.

Discussion

This study shows that ATP is required for maintaining operational $Ca_V1.3$ Ca^{2+} influx in IHCs via efficient Ca^{2+} clearance to secure sufficiently low basal $[Ca^{2+}]_i$ and avoid steady-state CDI.

ATP dependence of IHC $Ca_V1.3$

The role of ATP in the regulation of L-type Ca^{2+} channels varies among cells of different tissues. First, phosphorylation/dephosphorylation have been shown to regulate channel gating (Xu et al., 2004). Second, ATP may alter Ca^{2+}-dependent proteases, which directly interact with the Ca^{2+} channel (Altier et al., 2011). Finally, lack of ATP leads to failure of ATP-dependent Ca^{2+} pumps and to cytosolic Ca^{2+} accumulation that may trigger CDI of Ca^{2+} channels (Belles et al., 1988; von Gersdorff and Matthews, 1996).

Based on the present work using potent kinase inhibitors, a modulation of the IHC $Ca_V1.3$ channel by phosphorylation via CaMKII is unlikely. The majority of protein kinases (including CaMKII and PKA) can use ATP-γ-S, although it is a poorer substrate than ATP (Palvimo et al., 1985; Ishida et al., 1996), further arguing against an implication of CaMKII- and PKA-mediated phosphorylation in the ATP-γ-S-induced I_{Ca} reduction. Interestingly, it has been suggested that ATP-γ-S supports the normal function of $Ca_V1.4$ channels in synaptic terminals of bipolar cells by serving kinases as a substrate for thiophosphorylation (Heidelberger et al., 2002). In this context, the better maintained I_{Ca} in recordings with ATP-γ-S compared with those without exogenous ATP together with the mild effect on I_{Ca} of the PKA inhibitor KT5720 may indicate a modest positive effect of PKA-mediated phosphorylation of $Ca_V1.3$ on IHC I_{Ca}.

Steady-state CDI of $Ca_V1.3$ channels by elevated resting $[Ca^{2+}]$ in IHCs

Parallel measurements of IHC $[Ca^{2+}]$ and I_{Ca} revealed a coincident and correlated increase of resting $[Ca^{2+}]$ and I_{Ca} inactiva-

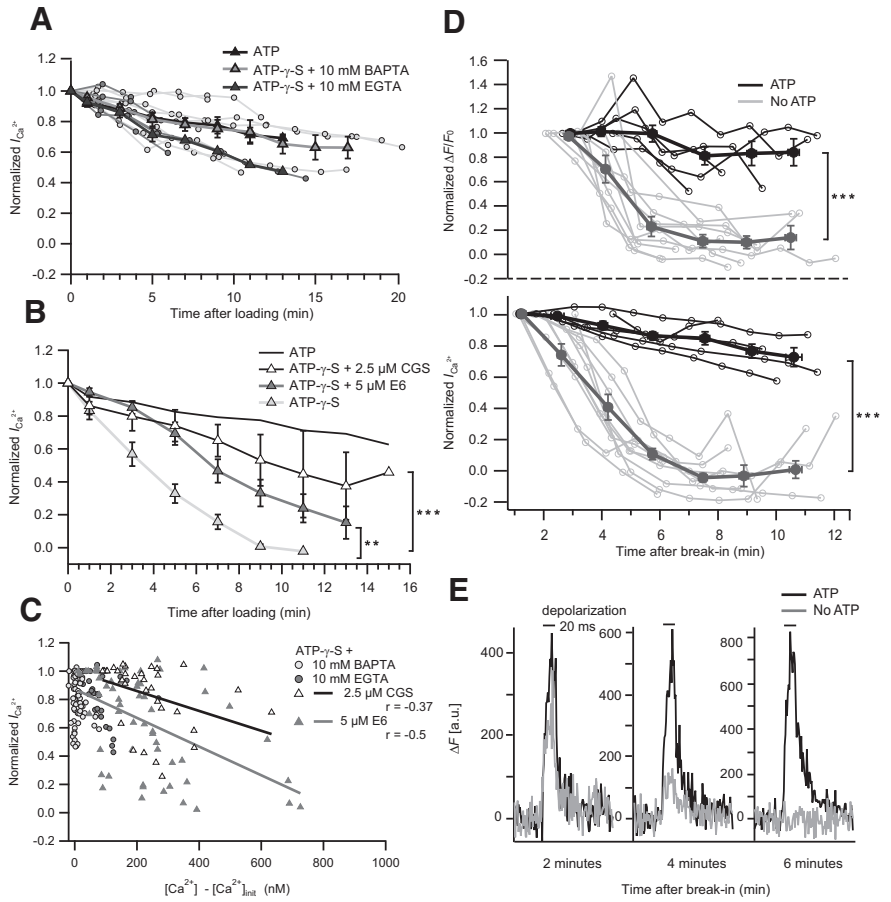

Figure 4. Ca^{2+} chelators and CaM inhibitors prevent I_{Ca} rundown; synaptic Ca^{2+} signaling requires ATP. ***A***, Normalized I_{Ca} of single IHCs dialyzed with 2 mM ATP-γ-S and either 10 mM EGTA ($n = 6$) or 10 mM BAPTA ($n = 9$). Normalized mean I_{Ca} overlaid. For comparison, the mean normalized I_{Ca} of control IHCs is displayed (black solid line). ***B***, The mean normalized I_{Ca} of IHCs dialyzed with 2 mM ATP-γ-S and 0.5 mM EGTA in the absence ($n = 10$) or presence of berbamine E_6 ($n = 9$) or CGS-9343B ($n = 8$) as well as control IHCs (2 mM ATP, $n = 5$). Statistical comparison was performed between 3 and 9 min after loading. ***C***, Correlation between I_{Ca} and basal $[Ca^{2+}]_i$ of ATP-γ-S-infused IHCs is weaker in the presence of CaM inhibitors (compare with Fig. 3*D*) and absent with high buffer concentrations. ***D***, Rundown of synaptic Ca^{2+} signals at IHC AZs in the absence of ATP. Normalized $\Delta F/F_0$ (top) of Fluo-4FF at an AZ and normalized I_{Ca} (bottom) of the same IHCs in the presence ($n = 5$) and absence ($n = 10$) of 2 mM ATP in the pipette solution. Thick lines indicate mean ± SEM (bin size, 100 s); thin lines indicate individual traces. Statistical comparison was performed between 4 min and 12 min after break-in. The initial data points of $\Delta F/F_0$ were omitted because of noise introduced by low F_0. ***E***, Decreasing amplitude of AZ Ca^{2+} signal in the absence of ATP. Temporal profiles of Fluo-4FF fluorescence at two exemplary AZs in the presence (black) and absence (gray) of 2 mM ATP during 20 ms depolarization (black bars) at 2, 4, and 6 min after break-in. $^{**}p < 0.01$. $^{***}p < 0.001$.

tion in the absence of hydrolyzable ATP or pharmacological block of PMCAs in IHCs. PMCAs are the major source of Ca^{2+} extrusion from IHCs (Kennedy, 2002) and other cells with ribbon synapses (Zenisek and Matthews, 2000). Lack of ATP or its hydrolysis (ATP-γ-S) (Eckstein, 1985) disables their pumping activity; indeed, the ATP-γ-S-mediated global Ca^{2+} increase observed in IHCs could be mimicked by the PMCA inhibitor CE. These findings emphasize the essential role of PMCA-mediated Ca^{2+} clearance for synaptic transmission. In addition to PMCA endogenous immobile and mobile Ca^{2+} buffers, the latter estimated at 0.5–1 mM Ca^{2+} binding sites (Hackney et al., 2005; Johnson and Marcotti, 2008) have been proposed to shape synaptic Ca^{2+} signals in IHCs (Frank et al., 2009). Our results suggest that, in conditions of metabolic stress that lowers the cytosolic ATP levels (likely 1–2 mM in hair cells) (Puschner and Schacht, 1997; Shin et al., 2007), IHCs may fail to maintain low resting $[Ca]_i$ and normal I_{Ca}, which would then impede sensory signaling during prolonged stimulation.

Steady-state CDI driven by enhanced basal cytosolic Ca^{2+} has been documented for Ca_V channels of cardiomyocytes and retinal bipolar cells (Belles et al., 1988; von Gersdorff and Matthews, 1996). In the latter, the dialysis with elevated Ca^{2+} led to a block of I_{Ca}. In the present study, we corroborated our hypothesis that the absence of hydrolyzable ATP triggers steady-state CDI in IHCs via increased basal cytosolic Ca^{2+} by showing that EGTA, BAPTA, and the calmodulin inhibitors antagonize the I_{Ca} rundown. Work on the molecular mechanism of Ca^{2+}/calmodulin modulation of the C terminus of the Ca_V channels indicates that the N-terminal lobe of CaM might respond preferentially to the global accumulation of Ca^{2+} (Dick et al., 2008). IHCs use several mechanisms to counteract CDI. An increase of steady-state inactivation of $Ca_V1.3$ channels in IHCs, as found here upon manipulation of the ATP supply, is expected to reduce the rate of transmitter release and, consequently, of spiking in the postsynaptic spiral ganglion neurons. Interestingly, a human mutation in the gene coding for Ca^{2+} binding protein 2 that antagonizes CDI impairs hearing (Schrauwen et al., 2012) potentially because of increased steady-state inactivation. It is conceivable that IHC Ca^{2+} influx, synaptic sound coding, and hearing can be compromised also by other mechanisms that lead to enhanced CDI, and the metabolic state of the IHC may couple to sound encoding via the mechanism described in this study.

References

Altier C, Garcia-Caballero A, Simms B, You H, Chen L, Walcher J, Tedford HW, Hermosilla T, Zamponi GW (2011) The Cavβ subunit prevents RFP2-mediated ubiquitination and proteasomal degradation of L-type channels. Nat Neurosci 14:173–180. CrossRef Medline

Armstrong D, Eckert R (1987) Voltage-activated calcium channels that must be phosphorylated to respond to membrane depolarization. Proc Natl Acad Sci U S A 84:2518–2522. CrossRef Medline

Asano S, Komiya M, Koike N, Koga E, Nakatani S, Isobe Y (2010) 5,6,7,8-Tetrahydropyrido[4,3-d]pyrimidines as novel class of potent and highly selective CaMKII inhibitors. Bioorg Med Chem Lett 20:6696–6698. CrossRef Medline

Basavappa S, Mangel AW, Scott L, Liddle RA (1999) Activation of calcium channels by cAMP in STC-1 cells is dependent upon Ca^{2+} calmodulin-dependent protein kinase II. Biochem Biophys Res Commun 254:699–702. CrossRef Medline

Belles B, Malécot CO, Hescheler J, Trautwein W (1988) "Run-down" of the Ca current during long whole-cell recordings in guinea pig heart cells: role of phosphorylation and intracellular calcium. Pflugers Arch 411:353–360. CrossRef Medline

Brandt A, Striessnig J, Moser T (2003) CaV1.3 channels are essential for development and presynaptic activity of cochlear inner hair cells. J Neurosci 23:10832–10840. Medline

Brandt A, Khimich D, Moser T (2005) Few CaV1.3 channels regulate the

exocytosis of a synaptic vesicle at the hair cell ribbon synapse. J Neurosci 25:11577–11585. CrossRef Medline

Chad JE, Eckert R (1986) An enzymatic mechanism for calcium current inactivation in dialysed Helix neurones. J Physiol 378:31–51. Medline

Chijiwa T, Mishima A, Hagiwara M, Sano M, Hayashi K, Inoue T, Naito K, Toshioka T, Hidaka H (1990) Inhibition of forskolin-induced neurite outgrowth and protein phosphorylation by a newly synthesized selective inhibitor of cyclic AMP-dependent protein kinase, N-[2-(p-bromocinnamylamino)ethyl]-5-isoquinolinesulfonamide (H-89), of PC12D pheochromocytoma cells. J Biol Chem 265:5267–5272. Medline

Cui G, Meyer AC, Calin-Jageman I, Neef J, Haeseleer F, Moser T, Lee A (2007) Ca^{2+}-binding proteins tune Ca^{2+}-feedback to Cav1.3 channels in mouse auditory hair cells. J Physiol 585:791–803. CrossRef Medline

Dick IE, Tadross MR, Liang H, Tay LH, Yang W, Yue DT (2008) A modular switch for spatial Ca^{2+} selectivity in the calmodulin regulation of CaV channels. Nature 451:830–834. CrossRef Medline

Dou H, Vazquez AE, Namkung Y, Chu H, Cardell EL, Nie L, Parson S, Shin HS, Yamoah EN (2004) Null mutation of alpha1D Ca^{2+} channel gene results in deafness but no vestibular defect in mice. J Assoc Res Otolaryngol 5:215–226. CrossRef Medline

Eckstein F (1985) Nucleoside phosphorothioates. Annu Rev Biochem 54:367–402. CrossRef Medline

Francis AA, Mehta B, Zenisek D (2011) Development of new peptide-based tools for studying synaptic ribbon function. J Neurophysiol 106:1028–1037. CrossRef Medline

Frank T, Khimich D, Neef A, Moser T (2009) Mechanisms contributing to synaptic Ca^{2+} signals and their heterogeneity in hair cells. Proc Natl Acad Sci U S A 106:4483–4488. CrossRef Medline

Grant L, Fuchs P (2008) Calcium- and calmodulin-dependent inactivation of calcium channels in inner hair cells of the rat cochlea. J Neurophysiol 99:2183–2193. CrossRef Medline

Grynkiewicz G, Poenie M, Tsien RY (1985) A new generation of Ca^{2+} indicators with greatly improved fluorescence properties. J Biol Chem 260:3440–3450. Medline

Hackney CM, Mahendrasingam S, Penn A, Fettiplace R (2005) The concentrations of calcium buffering proteins in mammalian cochlear hair cells. J Neurosci 25:7867–7875. CrossRef Medline

Heidelberger R, Sterling P, Matthews G (2002) Roles of ATP in depletion and replenishment of the releasable pool of synaptic vesicles. J Neurophysiol 88:98–106. Medline

Ishida A, Kitani T, Fujisawa H (1996) Evidence that autophosphorylation at Thr-286/Thr-287 is required for full activation of calmodulin-dependent protein kinase II. Biochim Biophys Acta 1311:211–217. CrossRef Medline

Issa NP, Hudspeth AJ (1996) The entry and clearance of Ca^{2+} at individual presynaptic active zones of hair cells from the bullfrog's sacculus. Proc Natl Acad Sci U S A 93:9527–9532. CrossRef Medline

Johnson SL, Marcotti W (2008) Biophysical properties of CaV1.3 calcium channels in gerbil inner hair cells. J Physiol 586:1029–1042. Medline

Kennedy HJ (2002) Intracellular calcium regulation in inner hair cells from neonatal mice. Cell Calcium 31:127–136. CrossRef Medline

Lee A, Wong ST, Gallagher D, Li B, Storm DR, Scheuer T, Catterall WA (1999) Ca^{2+}/calmodulin binds to and modulates P/Q-type calcium channels. Nature 399:155–159. CrossRef Medline

Mammano F, Bortolozzi M, Ortolano S, Anselmi F (2007) Ca^{2+} signaling in the inner ear. Physiology (Bethesda) 22:131–144. CrossRef Medline

Moser T, Beutner D (2000) Kinetics of exocytosis and endocytosis at the cochlear inner hair cell afferent synapse of the mouse. Proc Natl Acad Sci U S A 97:883–888. CrossRef Medline

Neher E (2013) Measurement of calibration constants for quantitative calcium fluorimetry. Cold Spring Harb Protoc 2013:947–948. CrossRef Medline

Norman JA, Ansell J, Stone GA, Wennogle LP, Wasley JW (1987) CGS 9343B, a novel, potent, and selective inhibitor of calmodulin activity. Mol Pharmacol 31:535–540. Medline

Ohya Y, Sperelakis N (1989) Modulation of single slow (L-type) calcium channels by intracellular ATP in vascular smooth muscle cells. Pflugers Arch 414:257–264. CrossRef Medline

Okada Y, Sato-Yoshitake R, Hirokawa N (1995) The activation of protein kinase A pathway selectively inhibits anterograde axonal transport of vesicles but not mitochondria transport or retrograde transport in vivo. J Neurosci 15:3053–3064. Medline

Palvimo J, Linnala-Kankkunen A, Mäenpää PH (1985) Thiophosphorylation and phosphorylation of chromatin proteins from calf thymus in vitro. Biochem Biophys Res Commun 126:103–108. CrossRef Medline

Peterson BZ, DeMaria CD, Adelman JP, Yue DT (1999) Calmodulin is the Ca^{2+} sensor for Ca^{2+}-dependent inactivation of L-type calcium channels. Neuron 22:549–558. CrossRef Medline

Platzer J, Engel J, Schrott-Fischer A, Stephan K, Bova S, Chen H, Zheng H, Striessnig J (2000) Congenital deafness and sinoatrial node dysfunction in mice lacking class D L-type Ca^{2+} channels. Cell 102:89–97. CrossRef Medline

Pusch M, Neher E (1988) Rates of diffusional exchange between small cells and a measuring patch pipette. Pflugers Arch 411:204–211. CrossRef Medline

Puschner B, Schacht J (1997) Energy metabolism in cochlear outer hair cells in vitro. Hear Res 114:102–106. CrossRef Medline

Roberts WM (1993) Spatial calcium buffering in saccular hair cells. Nature 363:74–76. CrossRef Medline

Schrauwen I, Helfmann S, Inagaki A, Predoehl F, Tabatabaiefar MA, Picher MM, Sommen M, Seco CZ, Oostrik J, Kremer H, Dheedene A, Claes C, Fransen E, Chaleshtori MH, Coucke P, Lee A, Moser T, Van Camp G (2012) A mutation in CABP2, expressed in cochlear hair cells, causes autosomal-recessive hearing impairment. Am J Hum Genet 91:636–645. CrossRef Medline

Shin JB, Streijger F, Beynon A, Peters T, Gadzala L, McMillen D, Bystrom C, Van der Zee CE, Wallimann T, Gillespie PG (2007) Hair bundles are specialized for ATP delivery via creatine kinase. Neuron 53:371–386. CrossRef Medline

Singh A, Gebhart M, Fritsch R, Sinnegger-Brauns MJ, Poggiani C, Hoda JC, Engel J, Romanin C, Striessnig J, Koschak A (2008) Modulation of voltage- and Ca^{2+}-dependent gating of CaV1.3 L-type calcium channels by alternative splicing of a C-terminal regulatory domain. J Biol Chem 283:20733–20744. CrossRef Medline

Sumi M, Kiuchi K, Ishikawa T, Ishii A, Hagiwara M, Nagatsu T, Hidaka H (1991) The newly synthesized selective Ca^{2+}/calmodulin dependent protein kinase II inhibitor KN-93 reduces dopamine contents in PC12h cells. Biochem Biophys Res Commun 181:968–975. CrossRef Medline

Tucker T, Fettiplace R (1995) Confocal imaging of calcium microdomains and calcium extrusion in turtle hair cells. Neuron 15:1323–1335. CrossRef Medline

von Gersdorff H, Matthews G (1996) Calcium-dependent inactivation of calcium current in synaptic terminals of retinal bipolar neurons. J Neurosci 16:115–122. Medline

Xu JJ, Hao LY, Kameyama A, Kameyama M (2004) Calmodulin reverses rundown of L-type Ca(2+) channels in guinea pig ventricular myocytes. Am J Physiol Cell Physiol 287:C1717–C1724. CrossRef Medline

Yang PS, Alseikhan BA, Hiel H, Grant L, Mori MX, Yang W, Fuchs PA, Yue DT (2006) Switching of Ca^{2+}-dependent inactivation of Ca(v)1.3 channels by calcium binding proteins of auditory hair cells. J Neurosci 26:10677–10689. CrossRef Medline

Zenisek D, Matthews G (2000) The role of mitochondria in presynaptic calcium handling at a ribbon synapse. Neuron 25:229–237. CrossRef Medline